Magnetic properties of vapor-deposited iron–noble-metal multilayers

B. X. Liu and F. Pan
Department of Materials Science and Engineering, Tsinghua University, Beijing 100084, China and Center of Condensed Matter and Radiation Physics, Chinese Center of Advanced Science and Technology (World Laboratory), Beijing 100080, China
(Received 26 April 1993)

A vapor-deposition technique was employed to investigate the magnetic properties of iron–noble-metal multilayers. The thickness, periodicity, chemical composition, microstructure, and the magnetic moment of the films were characterized and measured by various methods. The experimental results indicated that the magnetic moment per Fe atom in iron–noble-metal multilayers was significantly enhanced with decreasing Fe-layer thickness, with a fixed noble-metal thickness. The magnetic enhancement was found to be up to 120% for Fe(4.5 nm)/Au(7.5 nm), 120% for Fe(1.2 nm)/Ag(9 nm), and 160% for Fe(1.5 nm)/Cu(7.5 nm) multilayers, respectively, within an error of 6%. Also, when the thickness of the Fe layer decreased, there was an increasing tendency for perpendicular magnetization in the iron–noble-metal multilayers. The possible mechanism of the magnetic-moment enhancement is discussed in terms of the metastable atomic configuration of Fe atoms at the iron–noble-metal interfaces.

I. INTRODUCTION

In the last few years, magnetic multilayer films on a nanometer scale with artificial periodicity have attracted much attention because these films have the possibility of exhibiting anomalous magnetic properties, e.g., the change in magnetization as the magnetic layer thickness is reduced and the appearance in some cases of a uniaxial interfacial anisotropy, etc. The iron–noble-metal multilayers have been the most extensively studied systems,[1–5] because these systems have the advantage of a good lattice match, which reduces interfacial strain, and iron–noble-metal mutlilayers have weak electronic coupling between and unique chemical protection when the noble-metal layers are deposited on top.

Based on an all-electron total energy local spin density approach, Freeman and co-workers[6–8] predicted that there would be a significant enhancement in the two-dimensional (2D) magnetism at surfaces and interfaces in transition metals on noble metals, e.g., the magnetic moment of the Fe atom, in comparison to its value of 2.15 μ_B in bulk Fe, could be up to 2.98 μ_B for the topmost Fe overlayer and the clean Fe(001) surface, 2.96 μ_B for a monolayer of Fe/Ag(001), 2.85 μ_B for a monolayer of Fe/Cu(001), 2.80 μ_B for the Ag/Fe/Ag(001) sandwich, and 2.92 μ_B for the Au/Fe/Au(001) sandwich, respectively. Tight-binding calculations of the magnetic properties of surface, interface, and multilayers by Krompiewski, Krauss, and Krey,[9] Tersoff and Falicov,[10] and Falicov, Victora, and Terrsoff,[11] gave a similar prediction; e.g., Krompiewski, Krauss, and Krey[9] predicted that the magnetic moment of Fe/Ag multilayers could be up to 2.86 μ_B by adopting an atomic sphere approximation and using a first principle tight-binding linear muffin-tin orbital method. Similarly, Maclaren *et al.*[12] predicted that the magnetic moment of Fe/Au superlattices and interfaces could be up to 2.78 μ_B by a spin-polarized layer Korringa-Kohn-Rostoker method. In short, from the theoretical calculations, the magnetic moment per Fe atom could be enhanced up to 130% to 140% in thin films. Besides, these calculations, also made a prediction for a tendency of out-of-plane (perpendicular) magnetic anisotropy, because of the very weak coupling in Fe–noble-metal systems.

From the experimental results reported in the literature, however, considerable enhancement of magnetic moment of Fe atoms has not yet been observed, though iron–noble-metal multilayers have been studied by many research groups,[2–5,13–18] instead only a slight enhancement of magnetic moment in Fe/Ag superlattice and multilayers has been shown recently.[19,20] It is believed that different preparation techniques would result in different morphologies at the interface of the prepared multilayers and thus modify the magnetization differently. In those previous studies, the iron–noble-metal mutlilayers were prepared by ion sputtering and magnetron sputtering techniques, which probably resulted in a rough interface or even interfacial mixing, as the sputtered atoms were quite energetic. These results can therefore not match the calculations based on an ideal magnetic and/or nonmagnetic interface. Very recently, Himpsel[1] and Macedo, Keune, and Ellerbrock[21] reported that Fe grew epitaxially in an fcc structure on Cu single crystals and formed a sharp interface. In our recent study,[22] it was also found that Fe grew epitaxially on polycrystalline Cu by electron-beam (electron-gun) vapor deposition, in which the energy possessed by the evaporated atoms was considerably lower than those in previously reported techniques. A vapor-deposition technique was therefore employed to conduct a systematic study of the magnetic properties of the Fe/noble-metal systems. In this paper, we report the experimental results of magnetic-moment enhancement observed in the iron–noble-metal multilayers prepared by electron-gun vapor deposition, the correlation between the magnetic properties and the microstructure of the films, and discuss the possible mechanism responsible for the observed magnetic properties.

II. EXPERIMENTAL PROCEDURE

The iron–noble-metal multilayered films were prepared by depositing alternatively pure iron (99.99%) and noble-metal (Cu, Ag, and Au; 99.99%) at rates of 0.1–0.2 nm/s onto a NaCl single-crystal with a freshly cleaved surface (for microstructure analysis) and glass substrates of 0.1 mm thick (for magnetic property measurement) in an electron-gun evaporation system with a vacuum of 5×10^{-5} Pa. The thickness of the constituent metals varied from 1.2 to 12 nm controlled by an *in situ* quartz oscillator in the system. The total thickness and geometrical parameters of the multilayers are listed in Table I. Rutherford backscattering (RBS) was employed to measure the thickness and the periodicity of the samples. The samples were also analyzed by transmission electron microscopy (TEM), selected area electron diffraction (SAD), and x-ray diffraction to identify the structure of the films. The magnetic properties were measured with a vibrating-sample magnetometer (VSM) with a resolution of 2×10^{-6} emu under a magnetic field of 4 kOe at room temperature. The size of the VSM samples was 5 mm×5 mm. Since the measurements of the total magnetic moment of the films and the content of the Fe in the samples are of vital importance in calculating the magnetic moment per Fe atom, some precautions were taken. The hysteresis loop of the substrate and holder was first measured and the largest magnetic moment of the substrate and the holder was about 4×10^{-4} emu, which was about 1–2 orders of magnitude lower than that of the iron–noble-metal multilayers to be shown below. The hysteresis loops of iron–noble-metal multilayers were then measured and the magnetization of the substrate and holder was subtracted automatically by the computer during measuring. To reduce measuring error, four same specimens were put together in one measurement to obtain the hysteresis loops. Consequently, interference of the magnetic moment from the substrate and holder has a negligible effect on the measured values and the precision of the measured magnetic moment of the films was estimated to be less than 1%. After measuring the magnetic properties, the alloy films were dissolved in 5 ml *aqua regia* (HNO_3:HCl=1:3) and PLASMA-SPEC-I inductive coupled plasma (ICP) atomic emission spectrum was employed to determine the real Fe content in the multilayers. An average magnetic moment per Fe atom was then calculated using the obtained data. Taking into account of an error involved in the ICP measurement being 5%, the total measured error of the magnetic moment per Fe atom was reasonably estimated to be around 6%.

III. RESULTS AND DISCUSSION

A. Determination of the periodicity

RBS was used to verify the thickness and the periodicity of the iron–noble-metal multilayers. The experimental results indicated that the thickness and periodicity of all samples agreed well with our nominal values (Table I). For example, Figs. 1(a) and 1(b) show the Rutherford backscattering spectra of [Fe(11 nm)/Au (9 nm)]$_7$ (the subscript is the periodicity number of the Fe/Au bilayers and is the same hereafter) and [Fe(8 nm)/Au(7.5 nm)]$_8$ multilayers, respectively. The spectra were obtained with 2.1 MeV He^+ ions and the laboratory backscattering angle was 165°. From the spectra, one can learn that the peak corresponding to the high channel is the peak of gold or silver and the low channel is the peak of iron, and both iron and noble-metal consisted of seven peaks for [Fe(11 nm)/Ag(9 nm)]$_7$ and eight peaks for [Fe(8 nm)/Au(7.5 nm)]$_8$ films, corresponding to seven Ag/Fe and eight Au/Fe bilayers in these two mutlilayers, respectively. The total thicknesses of the samples were about 140 nm for Fe/Ag multilayers and 125 nm for Fe/Au ones, respectively, by calculating the RBS spectra.

B. Magnetic properties

1. Fe-Au system

The VSM results indicated that all the iron–noble-metal multilayers in our experiment have an in-plane easy-axis magnetization. Figure 2 shows the hysteresis loops of four Fe/Au multilayers under a magnetic field of 4 kOe, which was parallel to the film plane. Table II and Fig. 3 show the magnetic moment per Fe atom in Fe/Au multilayered films as a function of Fe layer thickness. It can be observed from Fig. 3 that the magnetic moment per Fe atom in Fe/Au mutlilayers was about the same as in the bulk Fe when the Fe layer thickness was about 8 nm, and that the magnetic moment per Fe atom was considerably enhanced with decreasing Fe layer thickness and reached a highest value of 2.59 μ_B at an Fe layer

TABLE I. The geometrical parameters of the iron–noble-metal mutlilayers. (Note: t_{Fe} and t_{Cu} stand for the thickness of the Fe and Cu layers, respectively.)

Specimen	Fe layer thickness (nm)	Cu layer thickness (nm)	Total thickness (nm)
Fe/Cu films	1.5, 3.0, 4.5, 7.5, 12	7.5	75, 275
	$t_{Fe}=t_{Cu}$=1.5, 3.0, 4.5, 7.5, 12		75
Fe/Ag films	1.2, 2.5, 3.5, 5.6, 7.8	9	140
Fe/Au films	1.4, 2.5, 4.5, 8.0, 11	7.5	125

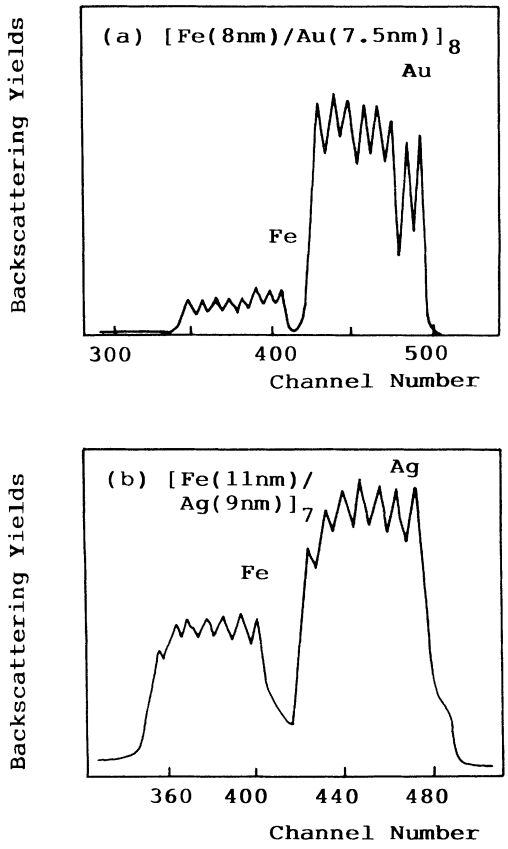

FIG. 1. RBS spectra of the iron–noble-metal mutlilayers. (a) $[Fe(8\ nm)/Au(7.5\ nm)]_8$ and (b) $[Fe(11\ nm)/Ag(9\ nm)]_7$ multilayers.

thickness of 4.7 nm, and then it slightly dipped with decreasing Fe layer thickness, while the Au layer was fixed at 7.5 nm in all the mutlilayers.

Figure 4 shows two hysteresis loops of the Fe/Au multilayers measured with the magnetic field parallel and perpendicular to the film plane, respectively. From the figure, it can be seen that the saturation magnetization field, for a perpendicular orientation, depended on the thickness of the Fe layer in a varying manner, when the Au layer was fixed at 7.5 nm. The saturation magnetization of the Fe(1.4 nm)/Au(7.5 nm) multilayers was much easier than that of the Fe(8 nm)/Au(7.5 nm) one. It was revealed that as the thickness of the Fe layer decreased, there was an increasing tendency for perpendicular magnetization in the Fe/Au mutlilayers, which was similar to that observed in Fe/Ag multilayers by Gutierrez, Mayer, and Walker.[17]

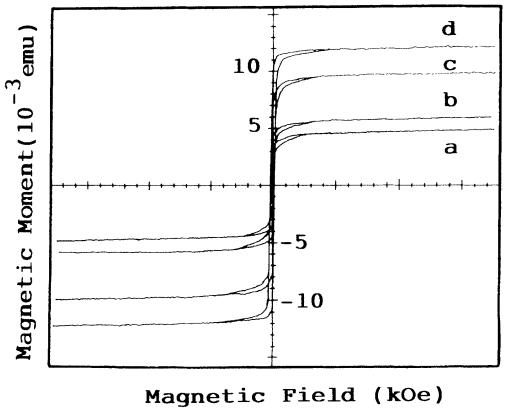

FIG. 2. The hysteresis loops of Fe/Au mutlilayers: (a) Fe(1.4 nm)/Au(7.5 nm); (b) Fe(2.5 nm)/Au(7.5 nm); (c) Fe(4.5 nm)/Au(7.5 nm); (d) Fe(8.0 nm)/Au(7.5 nm).

TABLE II. The magneic moment per Fe atom in different Fe/Au multilayers.

Specimen	σ_s (10^{-3} emu)	Weight of Fe (μg)	σ (μ_B)
Fe(1.4 nm)/Au(7.5 nm)	4.800	20.16	2.35
Fe(2.5 nm)/Au(7.5 nm)	5.967	24.65	2.39
Fe(4.5 nm)/Au(7.5 nm)	9.835	37.37	2.59
Fe(8.0 nm)/Au(7.5 nm)	12.22	55.51	2.17
Fe(11 nm)/Au(7.5 nm)	14.05	61.08	2.26
Bulk Fe			2.15

2. *Fe-Ag system*

The hysteresis lops of the Fe/Ag multilayers were also measured by the VSM to a maximum magnetic field of 4 kOe parallel to the film plane. The shape of the loops is similar to that of the Fe/Au multilayers. Table III and Fig. 5 show the magnetic moment per Fe atom in Fe/Ag multilayered films as a function of Fe layer thickness. From Fig. 5, it can be found that the magnetic moment per Fe atom in Fe/Ag multilayers was about the same as in the bulk Fe when the Fe layer thickness was about 11 nm, and that the magnetic moment per Fe atom was considerably enhanced with decreasing Fe layer thickness and reached 2.60 μ_B at an Fe layer thickness of 1.2 nm, while the Ag layer was fixed at 9 nm.

Figure 6 shows two hysteresis loops of the Fe/Ag multilayers measured with the magnetic field parallel and perpendicular to the film plane, respectively. From the figure, one sees that the saturation magnetization field

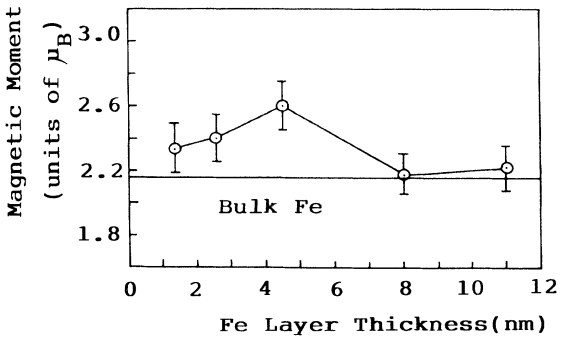

FIG. 3. Magnetic moment of Fe/Au multilayers as a function of the thickness of the Fe layer, while Au layer thickness was kept at 7.5 nm.

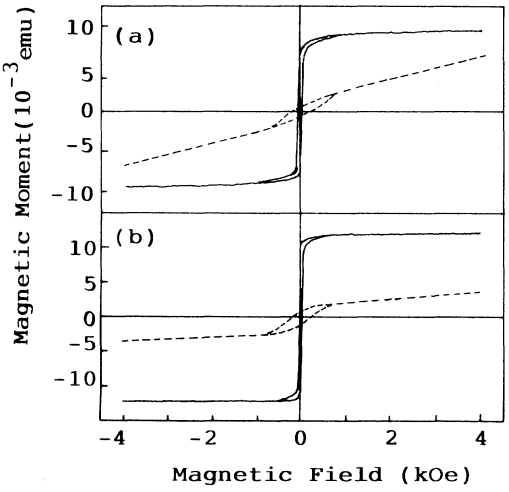

FIG. 4. The hysteresis loops measured in a magnetization field parallel (solid line) and perpendicular (dotted line) to the film plane for (a) Fe(1.4 nm)/Au(7.5 nm) and (b) Fe(8.0 nm)/Au(7.5 nm).

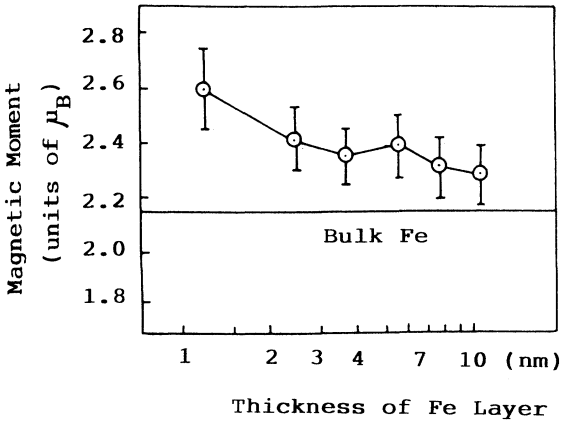

FIG. 5. Magnetic moment of Fe/Ag multilayers as a function of the thickness of the Fe layer, while Ag layer thickness was kept at 9 nm.

perpendicular to the film plane depended on the thickness of the Fe layer in a varying manner when the Ag layer was fixed at 9 nm. The saturation magnetization of the Fe(1.2 nm)/Ag(9 nm) multilayers was much easier than that of the Fe(11 nm)/Ag(9 nm). It was revealed that as the thickness of the Fe layer decreased, there was also an increasing tendency for perpendicular magnetization in the Fe/Ag multilayers similar to the above-mentioned Fe/Au mutlilayers.

3. *Fe-Cu system*

Table IV, Fig. 7, and Fig. 8 show the magnetic moment per Fe atom in Fe/Cu multilayered films as a function of Fe layer thickness. From Fig. 7, it can be seen that the magnetic moment per Fe atom in Fe/Cu mutlilayers was about the same as in the bulk Fe when the Fe layer was thicker than 7.5 nm, and that the magnetic moment per Fe atom was considerably enhanced with decreasing Fe layer thickness and reached 3.44 μ_B, i.e., about 1.6 times that of the bulk Fe, at an Fe layer thickness of 1.5 nm, while the Cu layer thickness was kept at 7.5 nm. The above magnetic properties of the Fe/Cu multilayers were measured with the specimens of a total thickness of 75 nm. We have studied the magnetic properties of the Fe/Cu multilayers of same periodicity but with a total thickness of 275 nm. Similar values of magnetic moment per Fe atom were obtained, implying that the total thickness and the Fe/Cu bilayer number have no detectable effect on the atomic magnetic moment. From Fig. 8, however, one can see that, when the thickness of the Fe layer is equal to that of the Cu and less than 7.5 nm, the magnetic moment per Fe atom weakened with decreasing Fe layer thickness, which was in agreement with the experimental results reported by Kozono *et al.*[13] Similar to the Fe/Au and Fe/Ag mutlilayers, there was also an increasing tendency for perpendicular magnetization in the Fe/Cu mutlilayers as the Fe thickness decreased.

TABLE III. The magnetic moment per Fe atom in different Fe/Ag multilayers.

Specimen	σ_s (10^{-3} emu)	Weight of Fe (μg)	σ (μ_B)
Fe(1.2 nm)/Ag(9 nm)	4.735	17.95	2.60
Fe(2.5 nm)/Ag(9 nm)	7.075	28.85	2.42
Fe(3.5 nm)/Ag(9 nm)	9.350	39.39	2.35
Fe(5.6 nm)/Ag(9 nm)	12.350	46.65	2.40
Fe(7.8 nm)/Ag(9 nm)	11.100	47.15	2.32

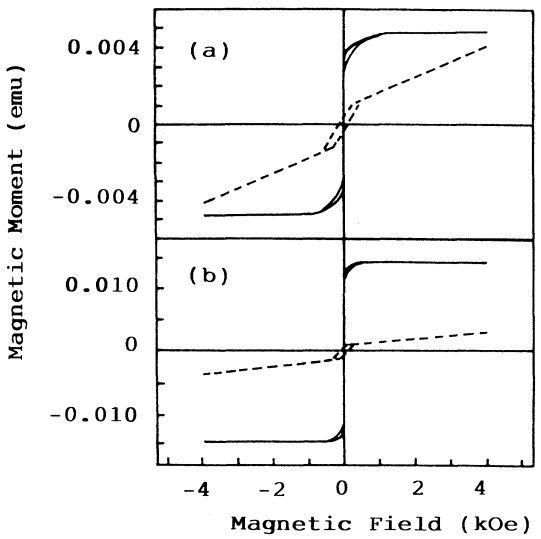

FIG. 6. The hysteresis loops measured in a magnetization field parallel (solid line) and perpendicular (dotted line) to the film plane for (a) Fe(1.2 nm)/Ag(9 nm) and (b) Fe(11 nm)/Ag(9 nm).

TABLE IV. The magnetic moment per Fe atom in different Fe/Cu multilayers.

Specimen	σ_s (10^{-3} emu)	Weight of Fe (μg)	σ (μ_B)
Fe(1.5 nm)/Cu(7.5 nm)	3.925	11.25	3.44
Fe(3.0 nm)/Cu(7.5 nm)	6.300	20.83	2.98
Fe(4.5 nm)/Cu(7.5 nm)	6.125	22.90	2.64
Fe(7.5 nm)/Cu(7.5 nm)	8.825	40.15	2.17
Fe(12 nm)/Cu(7.5 nm)	9.800	43.78	2.21
Fe(1.5 nm)/Cu(1.5 nm)	2.908	20.24	1.42
Fe(3.0 nm)/Cu(3.0 nm)	2.981	20.40	1.44
Fe(4.5 nm)/Cu(4.5 nm)	3.666	20.60	1.75
Fe(12 nm)/Cu(12 nm)	4.325	20.87	2.04

C. Microstructure analysis

1. Fe-Au system

To probe the reason of the magnetic-moment enhancement in the iron–noble-metal mutlilayers, the microstructure of the films was investigated by means of TEM SAD. The analysis results revealed that all the Fe/Au multilayers were composed of a mixture of the polycrystalline bcc Fe and fcc Au, and the size of the Fe and Au grains was smaller than 30 nm. Figure 9 shows a typical SAD pattern of the Fe(8 nm)/Au(7.5 nm) multilayers. From the intensity and distribution of the diffraction rings, it can be seen that the Au and Fe grains nucleated and grew homogeneously.

2. Texture relationship in Fe / Ag mutlilayers

Figure 10(a) shows a typical SAD pattern of the Fe(4.5 nm)/Ag(9 nm) multilayers taken at room temperature. From this figure, the diffraction rings of the sample were discontinuous, which was different from that of the Fe/Au mutlilayers, although the crystalline structure of Ag and Au was the same and their lattice parameters were very close (the difference is less than 0.2%). These results indicated that there were texture and specific

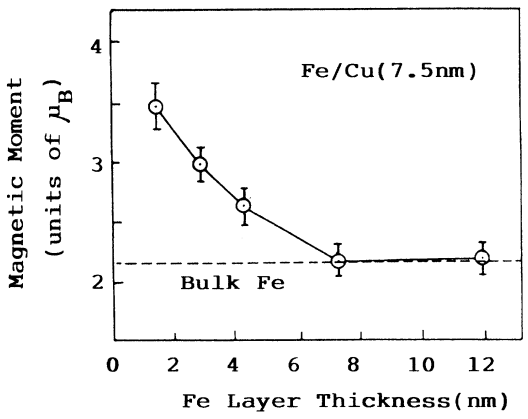

FIG. 7. Magnetic moment of Fe/Cu multilayers as a function of the thickness of the Fe layer, while Cu layer thickness was kept at 7.5 nm.

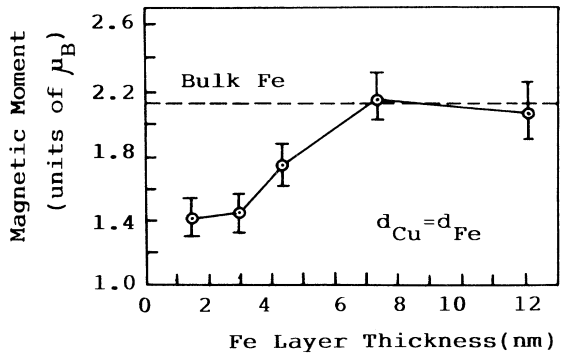

FIG. 8. Magnetic moment of Fe/Cu mutlilayers as a function of the thickness of the Fe layer, when the Cu layer thickness was the same as the Fe one.

orientation relationships emerging in the films. It was found by routine calculation that the (001) plane of most of the silver and iron grains was parallel to the film plane and that the (011) or (013) plane of some other silver grains was parallel to the film plane. From Fig. 10(a), it was figured out that there existed the following orientation relationships between most of silver and iron grains:

$$(001)_{Fe}\|(001)_{Ag}\ ,\quad [001]_{Fe}\|[110]_{Ag}\ ,$$

i.e., most of the Fe layers grew epitaxially on the (001) plane of the silver grains. A schematic diagram of an Fe/Ag bilayer is shown in Fig. 10(b). The reason of forming this texture may be that the atomic arrangement of the $(001)_{Fe}$ plane was almost the same as that of the $(001)_{Ag}$ plane and that Fe and Ag are essentially immiscible.

3. Epitaxial growth in Fe /Cu multilayers

The TEM SAD results revealed that, in the electron-beam vapor-deposited Fe/Cu mutlilayers, the microstructure of the Fe/Cu multilayers was apparently different from those of Fe/Au and Fe/Ag mutlilayers. Figure 11 shows four typical SAD patterns of the Fe/Cu multilayers with various Fe and Cu thicknesses. One sees from

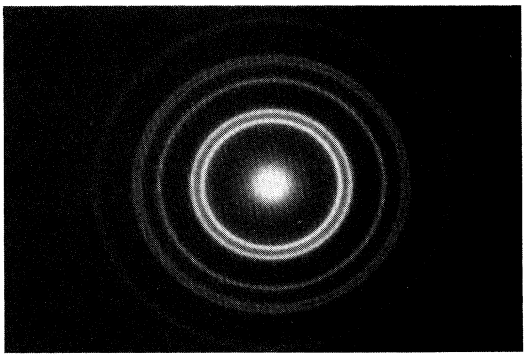

FIG. 9. Electron diffraction pattern of the Fe(8 nm)/Au(7.5 nm) mutlilayers.

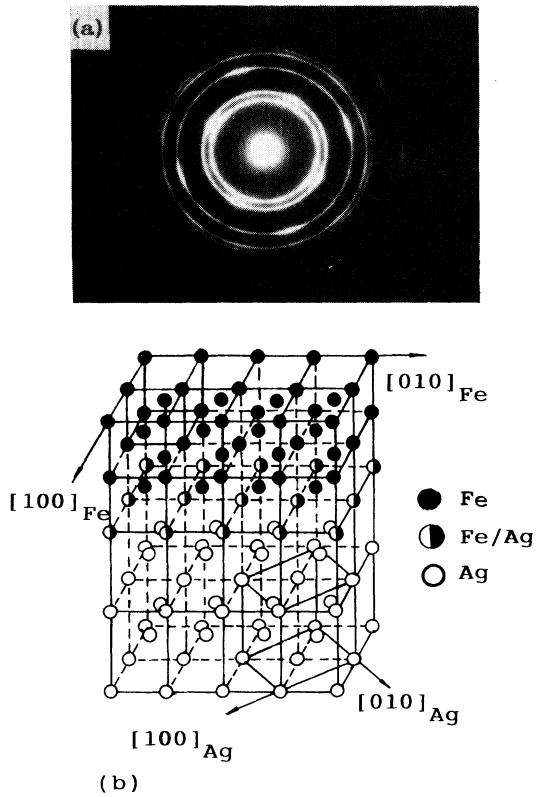

FIG. 10. (a) Electron diffraction pattern of the Fe(4.5 nm)/Ag(9 nm) mutlilayers; (b) a schematic diagram of an Fe/Ag bilayer.

the figure that when the thicknesses of Fe and Cu were very close, the diffraction intensity of bcc and fcc phase agreed with the proportion of the Fe and Cu contents. However, when Fe layer thickness was thinner than that of Cu, the diffraction intensity of the bcc Fe phase decreased sharply with decreasing Fe layer thickness. It was also true that, when the thickness of the Cu layer was thinner than that of Fe, the diffraction intensity of the fcc Cu phase decreased sharply with decreasing Cu layer thickness. Eventually, the diffraction lines from fcc Cu disappeared, when the thickness of the Cu and Fe layers were 3 and 12 nm, respectively. These results suggested that when the Cu layer was thinner than that of Fe, the crystalline structure of part of the Cu layer was not fcc but probably bcc, which grew epitaxially on polycrystalline Fe. It was also evident from SAD analysis that metastable fcc Fe grew epitaxially on polycrystalline Cu, when the Fe layer was thinner than that of Cu.

To provide further evidence of epitaxial growth of metastable bcc Cu or fcc Fe at the interfaces of Fe/Cu multilayers, the structural transformation of the films upon thermal annealing was studied by means of TEM and SAD. Figure 12 shows the SAD patterns of the Fe(9 nm)/Cu(3 nm) sample taken at room temperature and 350 °C, respectively. From the figure, the as-deposited film is composed of bcc and fcc phases; however, the intensities of the fcc Cu(200), (220), and (311) diffraction lines are very weak. When the sample was heated, the intensity of the fcc Cu diffraction lines increased with the increasing of annealing temperature up to about 350 °C, indicating an increasing portion of fcc Cu in the sample. Figure 13 shows the lattice parameter of the bcc Fe phase in Fe(9 nm)/Cu(3 nm) multilayers as a function of annealing temperature. From the figure, one sees that the lattice parameter in the as-deposited sample was 0.2895 nm, which was greater than that of bulk Fe (0.2866). Upon annealing, the lattice parameter of Fe first decreased with an increase of the annealing temperature until 350 °C, and then increased as usual when the temperature was higher than 350 °C. These observations imply that in the as-deposited Fe/Cu multilayers, there existed some strain between Fe and Cu layers, resulting in an expanded Fe lattice. When the sample was heated up to 350 °C, the strain between Fe and Cu lattices was released and the unusual lattice expansion of the Fe disappeared. These results supported the above argument that a certain portion of the Cu grew epitaxially on polycrystalline Fe with a bcc lattice when the Cu layer was very thin. Similar experiments indicated that the metastable fcc Fe grew epi-

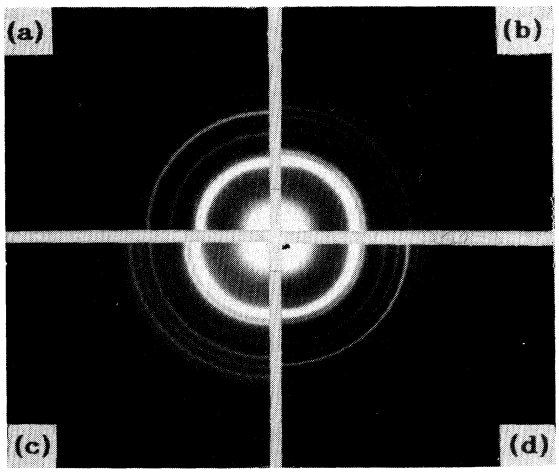

FIG. 11. Some typical diffraction patterns of the Fe/Cu mutlilayers (a) Fe(12 nm)/Cu(3 nm); (b) Fe(7.5 nm)/Cu(7.5 nm); (c) Fe(12 nm)/Cu(7.5 nm); (d) Fe(7.5 nm)/Cu(3 nm).

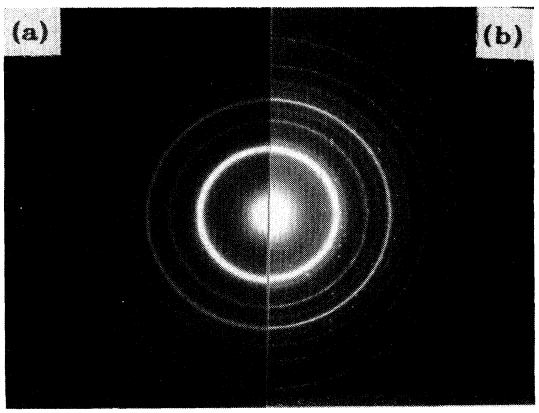

FIG. 12. The diffraction patterns of the Fe(9 nm)/Cu(3 nm) multilayers taken at (a) room temperature and (b) 350 °C.

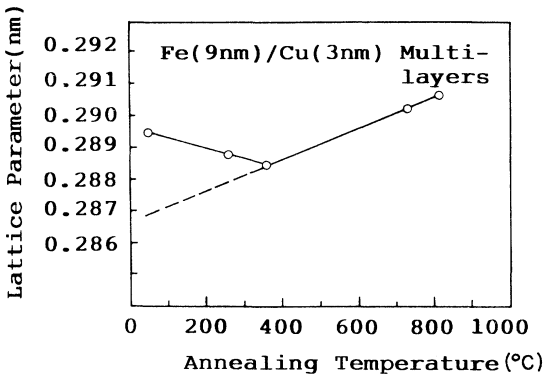

FIG. 13. The lattice parameter of the bcc Fe phase in Fe(9 nm)/Cu(3 nm) as a function of annealing temperature.

taxially on polycrystalline Cu in those films composing of thin Fe layer and thick Cu layer, and it transformed into equilibrium bcc phase after annealing at the appropriate temperature.

D. Discussion

The experimental results indicated that the magnetic properties of the iron noble-metal were determined by their microstructures, i.e., for different mutlilayers, the mechanism responsible for the modification of the magnetic properties might be different. In the Introduction, it was mentioned that the magnetic moment per Fe atom could be enhanced up to 130–140 % in thin-film form as predicted by various theoretical investigations, where most of these calculations were based on an ideal magnetic and/or nonmagnetic interface. In our experiments, the interface between magnetic layer and nonmagnetic layer in Fe/Cu multilayers could be considered to be an ideal situation as evidenced by the epitaxial growth of the metastable fcc Fe on a thick Cu layer. The above-mentioned calculations therefore explain the observed magnetic enhancement, when the Fe layer became very thin.

For Fe/Ag and Fe/Au mutlilayers, the Fe layer did not grow epitaxially on the fcc Ag or Au layer and retained its bcc structure. The mechanism of magnetic enhancement in Fe/Ag and Fe/Au mutlilayers was probably different from that in Fe/Cu mutlilayers. As predicted by Maclaren *et al.*[12] and McHenry and coworkers,[23,24] the observed magnetic enhancement of the Fe atoms in the Fe/Au and Fe/Ag multilayers may be interpreted by their calculation results based on the layer Korringa-Kohn-Rosoker method. An alternative explanation for the magnetic modification observed in the Fe/Ag multilayers may be attributed to the so-called interface "active layer" proposed by Krishinan and Tessier[20] and Krompiewski, Krauss, and Krey,[9] if such types of interface mixing layers really form. However, our experimental results of microstructure characterization are not adequate to make an appropriate explanation at present.

TABLE V. The relationship of the maximum magnetic moment per Fe atom in the iron–noble-metal multilayers with the difference of the covalent radius (Δr) between iron and noble metal (the covalent radius of the Fe atom is 0.117 nm).

Samples	$r_{\text{noble metal}}$ (nm)	$\Delta r / r_{\text{iron}}$ (%)	Magnetic moment (μ_B)
Fe(1.5 nm)/Cu(7.5 nm)	0.117	0	3.44
Fe(1.2 nm)/Ag(9 nm)	0.134	14.5	2.60
Fe(4.5 nm)/Au(7.5 nm)	0.134	14.5	2.59

It is of interest to note the relationship of the maximum magnetic moment per Fe atom in the iron–noble-metal multilayers with the difference of covalent radius between iron and noble metals (see Table V). For Fe/Cu films, the covalent radius of both Fe and Cu are 0.117 nm, i.e., the difference is 0. For Fe/Au and Fe/Ag films, the covalent radius of both Ag and Au are 0.134 nm and the difference of the covalent radius between Ag or Au and Fe is 0.017 nm. It seems that the maximum magnetic moment per Fe atom decreased with increasing the difference of the covalent radius. A small difference of the covalent radius may be favorable for epitaxial growth in the Fe/Cu multilayers. While for the Fe/Ag and Fe/Au mutlilayers the difference of the covalent radius was too big to let the Fe layer grow epitaxially. In the Fe-Ag system, the Fe atoms grew in a strong texture manner, while there was no structural coherency between the Fe and Au layers. The texture structure in Fe/Ag multilayers might play a secondary role in enhancing the magnetic moment and the maximum magnetic moment in Fe/Ag multilayers was slightly greater than that in Fe/Au ones.

In conclusion, our experimental results indicated that the magnetic moment of Fe atoms could be enhanced considerably in the Fe/noble-metal mutlilayers by employing a vapor-deposition technique. In the Fe/Cu case, because of the epitaxial growth of thin Fe layer on Cu, the magnetic enhancement was the highest one among three systems and could probably be explained by Freeman's calculation. In the Fe/Ag and Fe/Au cases, the magnetic enhancement was about 20%, which may be explained by some proposed theoretical predictions. While with decreasing Fe layer thickness, the increasing tendency for perpendicular magnetization is in accordance with those currently available theories.

ACKNOWLEDGMENTS

This work was support in part by the National Natural Science Foundation of China. The authors are grateful to the VSM Lab, TEM Lab, and Chemical Analysis Center of Peking University and the Institute of Materials Science of Tsinghua University for their assistance.

[1]F. J. Himpsel, Phys. Rev. Lett. **67**, 2363 (1991).
[2]H. Magnan, D. Chandesris, B. Villette, O. Heckmann, and J. Lecante, Phys. Rev. Lett. **67**, 859 (1991).
[3]D. G. Stinson and S.-C. Shin, J. Appl. Phys. **67**, 4459 (1990).
[4]T. Katayama, Y. Nishihara, and H. Awano, J. Appl. Phys. **61**, 4329 (1987).
[5]S. B. Qadri, C. Kim, M. Twigg, P. Lubitz, and M. Rubinstein, J. Vac. Sci. Technol. A **9**, 512 (1991).
[6]A. J. Freeman and C. L. Fu, J. Appl. Phys. **61**, 3356 (1987).
[7]C. L. Fu, A. J. Freeman, and T. Oguchi, Phys. Rev. Lett. **54**, 2700 (1985).
[8]E. Wimmer, A. J. Freeman, and H. Kradauer, Phys. Rev. B **30**, 3113 (1984).
[9]S. Krompiewski, U. Krauss, and U. Krey, J. Magn. Magn. Mater. **92**, L295 (1991).
[10]J. Tersoff and L. M. Falicov, Phys. Rev. B **26**, 6186 (1982).
[11]L. M. Falicov, R. H. Victora, and J. Tersoff, in *The Structure of Surfaces*, edited by M. A. Van Hove and S. Y. Tong (Springer, Heidelberg, 1985).
[12]J. M. Maclaren, M. E. McHenry, S. Crampin, and M. E. Eberhart, J. Appl. Phys. **67**, 5406 (1990).
[13]Y. Kozono, M. Komuro, S. Narishige, M. Hanazono, and Y. Sugita, J. Appl. Phys. **61**, 4311 (1987).
[14]F. Badia, G. Fratucello, B. Martinez, D. Fiorani, A. Labarta, and J. Tejada, J. Magn. Magn. Mater. **93**, 425 (1991).
[15]H. M. van Noort, F. J. A. den Broeder, and H. J. G. Draaisa, J. Magn. Magn. Mater. **51**, 273 (1985).
[16]Xiao-ding Ma, Lin-yuan Yang, Jian-gao Zhao, and Hui-qun Guo, J. Magn. Magn. Mater. **80**, 347 (1989).
[17]C. J. Gutierrez, S. H. Mayer, and J. C. Walker, J. Magn. Magn. Mater. **80**, 299 (1989).
[18]K. B. Urquhart, B. Heinrich, J. F. Cochran, A. S. Arrott, and K. Myrtle, J. Appl. Phys. **64**, 5334 (1988).
[19]J. Q. Xiao, A. Gavrin, Gang Xiao, J. R. Childress, W. A. Bryden, C. L. Chien, and A. S. Edelstein, J. Appl. Phys. **67**, 5388 (1990).
[20]R. Krishnan and M. Tessier, J. Appl. Phys. **67**, 5391 (1990).
[21]W. A. A. Macedo, W. Keune, and E. D. Ellerbrock, J. Magn. Magn. Mater **93**, 552 (1991).
[22]F. Pan, K. Tao, and B. X. Liu, Phys. Status Solidi A **132**, K35 (1992).
[23]M. E. McHenry, J. M. MacLaren, M. E. Eberhart, and S. Crampin, J. Magn. Magn. Mater. **88**, 134 (1990).
[24]M. E. McHenry and J. M. MacLarent, Phys. Rev. B **43**, 10 611 (1991).

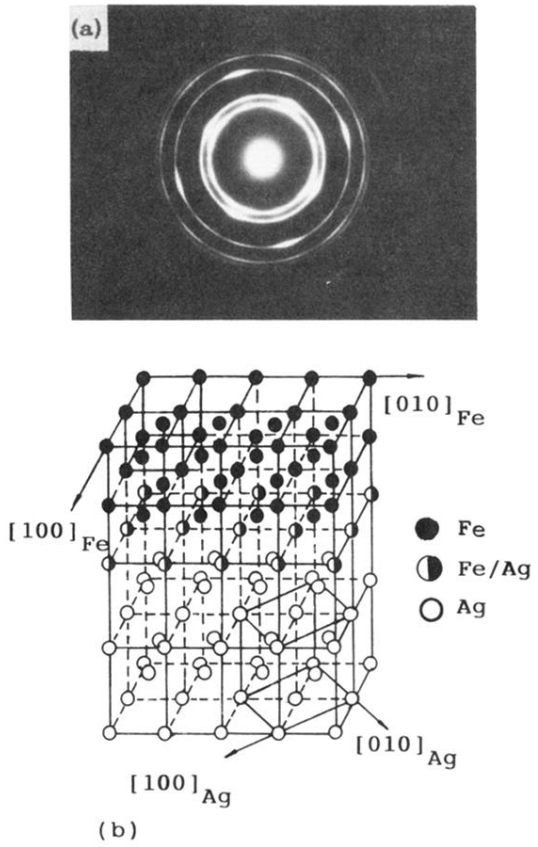

FIG. 10. (a) Electron diffraction pattern of the Fe(4.5 nm)/Ag(9 nm) mutlilayers; (b) a schematic diagram of an Fe/Ag bilayer.

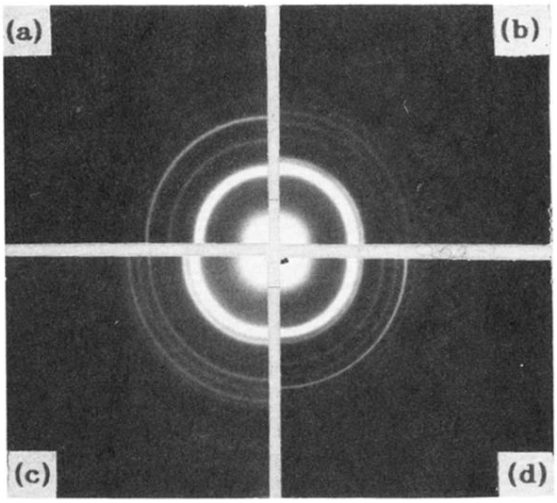

FIG. 11. Some typical diffraction patterns of the Fe/Cu mutlilayers (a) Fe(12 nm)/Cu(3 nm); (b) Fe(7.5 nm)/Cu(7.5 nm); (c) Fe(12 nm)/Cu(7.5 nm); (d) Fe(7.5 nm)/Cu(3 nm).

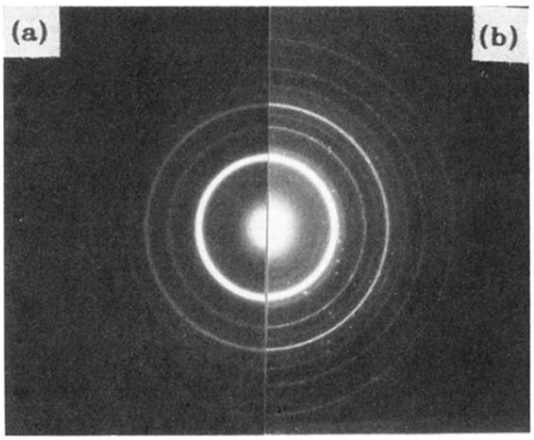

FIG. 12. The diffraction patterns of the Fe(9 nm)/Cu(3 nm) multilayers taken at (a) room temperature and (b) 350 °C.

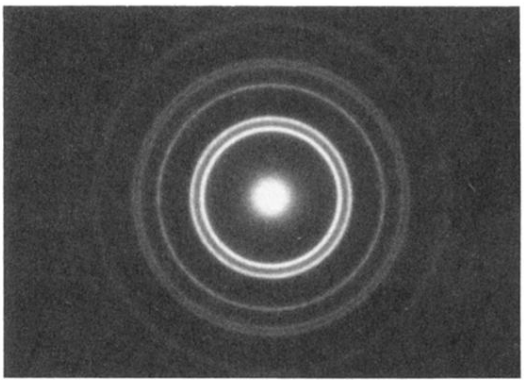

FIG. 9. Electron diffraction pattern of the Fe(8 nm)/Au(7.5 nm) mutlilayers.